AD NUMBER

AD234350

NEW LIMITATION CHANGE

TO

Approved for public release, distribution unlimited

FROM

Distribution authorized to U.S. Gov't. agencies and their contractors; Administrative/Operational Use; MAR 1960. Other requests shall be referred to Office of Naval Research, 800 North Quincy Street, Arlington, VA 22217-5660.

AUTHORITY

ONR ltr, 16 Feb 1979

U.S. NAVY
OFFICE OF NAVAL RESEARCH
WASHINGTON, D.C.

1 Copy

15 March 1960
Report No. 1772
(Final)
Copy No. AF-12-1

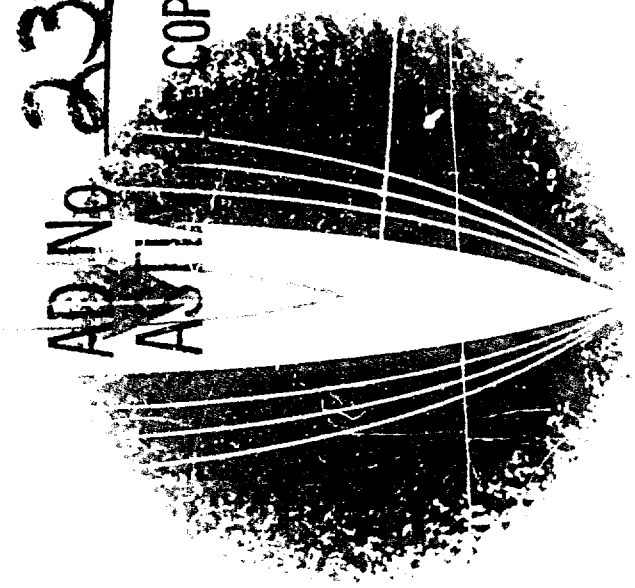

RESEARCH ON MECHANISMS OF DETONATION PROCESSES

Contract Nonr-2804(00)

Aerojet-General
GENERAL

15 March 1960

Report No. 1772
(Final)

RESEARCH ON MECHANISMS OF DETONATION PROCESSES

Contract Nonr 2804(00)

Written by:

R. F. Chaiken
K. J. Schneider

No. of Pages: 49

Period Covered:

1 February 1959 through 31 January 1960

Approved by:

E Mutchler for

D. L. Armstrong
Director of Chemistry

AEROJET-GENERAL CORPORATION

Azusa, California

ABSTRACT

Studies of the surface-decomposition characteristics and strong shock initiation of condensed explosives are described.

The surface decomposition of solid explosives has been studied directly by means of a hot-plate linear-pyrolysis technique and indirectly by means of the analysis of linear-burning-rate data. Toward this end, a special hot-plate pyrolysis apparatus has been designed and fabricated. Also, strands of pressed TNT have been prepared and burned in a Crawford bomb.

In addition to surface-decomposition studies, streak-camera studies of detonation initiation and propagation in explosives have been initiated. In particular, efforts have been directed toward measuring the reaction time of detonation when reaction is initiated by strong planar shock waves.

FOREWORD

The Aerojet-General Corporation, under the sponsorship of the Advanced Research Projects Agency (ARPA), through the Office of Naval Research, Contract Nonr 2804(00), initiated in 1959 a program of research on the mechanisms of detonation processes. This report summarizes the work carried out under that contract.

Much of this program of research is being continued under Contract AF 49(638)-851* with the Office of Scientific Research, and future work will be described in the reports issued under that contract.

*Supported in part by ARPA.

CONTENTS

CONTENTS (cont.)

I. OBJECTIVE

The objective of this investigation has been to obtain an understanding of the fundamental processes involved in the initiation and propagation of detonation, with particular emphasis on an elucidation of the kinetics of the chemical reactions which occur during the detonation of condensed explosives.

II. INTRODUCTION AND SUMMARY

The kinetic processes controlling the initiation, deflagration, and (nonideal) detonation of conventional solid high explosives (TNT, PETN, RDX, etc.) have never been isolated with certainty. Studies which have been conducted for many years have provided sufficient information to enable hypotheses to be reached regarding many observable explosive phenomena. It is, however, only within the last few years that the studies have become sufficiently quantitative to allow some definitive elaboration of these hypotheses.

There is strong evidence that, for all conventional high explosives, the initiation process is thermal in origin. Mechanical energy, such as a blow or friction, must be degraded into heat in order to ignite the explosive. Likewise, the energy of the shock wave preceding a detonation front in a solid explosive is degraded into heat by the work the shock does (by compression) on the explosive through which it is moving. On the assumption, then, that the initiation of an explosive is a thermal process, the overall characteristics of the initiation and propagation of detonation in explosives rest upon the balance between the thermal rate of energy release by conventional chemical reaction, and the rate of energy loss by gas expansion (mainly) and by thermal conductivity.

The mechanism of detonation in solid explosives may be conveniently considered from two broad aspects - viz., the surface properties and the bulk properties of the explosive. The various possible common detonation-reaction mechanisms, then, include the following:

A. GRAIN-BURNING

1. Gaseous diffusion is rate determining.

2. Bulk decomposition is rate determining.

3. Surface decomposition, evaporation, or sublimation is rate determining.

B. UNIMOLECULAR BULK DECOMPOSITION FROM SHOCK COMPRESSION

1. Unimolecular, first-order, bulk decomposition is rate determining.

2. Gaseous diffusion is rate determining.

A program undertaken to study the surface-decomposition characteristics and strong shock initiation of condensed explosives is reviewed in Section III.

The surface decomposition of solid explosives is being studied directly by means of a hot-plate linear-pyrolysis technique and indirectly by means of analysis of linear-burning-rate data. Toward this end, a special hot-plate pyrolysis apparatus has been designed and fabricated. Also, strands of pressed TNT have been prepared and burned in a Crawford bomb.

In addition to surface-decomposition studies, streak-camera studies of detonation initiation and propagation in explosives are being carried out. In particular, efforts are being made to measure the reaction time of detonation when reaction is initiated by strong planar shock waves.

III. TECHNICAL STATUS

A. SURFACE DECOMPOSITION OF EXPLOSIVES

1. Background

In the grain-burning theory, originally due to Eyring and his co-workers (Reference 1), the initiation and propagation of detonation in heterogeneous explosives are considered on a microscopic scale to proceed through a mechanism whereby chemical reaction is induced in and spreads from "hot spots" produced by localized stress from impact (e.g., shock or mechanical impact). Bowden and his co-workers were among the first to introduce the hot-spot concept (Reference 2).

The detonation reaction time (τ) is then given by

$$\tau = \frac{\bar{R}_g}{Lk_r} \quad \text{sec} \qquad (1)$$

where $\bar{R}_g$ is the average radius of the explosive particles in the grain, L is the effective diameter of a molecule on the surface of the grain, and k_r is the specific rate constant of the rate-controlling reaction. The value of L can be taken to be approximately $(M/\rho N)^{1/3}$, where M is the molecular weight of the explosive, ρ is the density, and N is Avogadro's number. The detailed energy-release mechanism in the grain-burning theory need not be known for an evaluation of detonation-reaction times; it is only necessary to isolate the rate-determining step.

The work of Andersen and Chaiken at Aerojet-General (References 3 and 4) demonstrated that (low-velocity) detonation in low-energy granular explosives, such as ammonium nitrate and ammonium perchlorate at low packing densities, could be achieved by the same rate-controlling chemical reactions as deflagration (References 5 and 6). It was shown, by extrapolating experimental, linear-pyrolysis-rate data for these compounds to detonation conditions, that reasonable reaction times could be calculated. It was concluded that the one uniquely rate-controlling reaction in grain-burning detonation is the linear, thermal, surface-gasification rate (or linear pyrolysis rate) of the explosive particles. This surface gasification usually will consist of an evaporation or sublimation process. Thus, the linear pyrolysis rate (B_s) is considered to be the proper value for Lk_r. By employing the experimental linear-pyrolysis-rate data for NH_4NO_3 and NH_4ClO_4, it was possible to calculate detonation-reaction times which were consistent (within experimental error) with those predicted by the nozzle and curved-front-diameter theories.

Under Contract Nonr 2804(00), work has been under way to test the extension of these concepts to high-energy explosives (e.g., TNT, PETN, and RDX).

2. Experimental Studies

a. In order to obtain linear-pyrolysis-rate data on high explosives, a special hot-plate apparatus has been designed and fabricated (Figures 1 and 2). The need for this special apparatus was based upon safety requirements for carrying out the desired surface-decomposition studies. In general, the basic design of the original apparatus (References 7 and 8) was followed. However, several desirable improvements were added (1) extending the environmental pressures obtainable to ~ 2000 psi, and (2) increasing the range of strand loading force which can be applied. It is expected that measurements of the linear pyrolysis rate of TNT and other solid explosives will soon be initiated.

b. In conjunction with the fabrication of the hot-plate apparatus, techniques have been developed to prepare sample strands of explosive by hydraulic ram pressing of the dry powder. Utilizing an Atlantic Research Corporation strand mold (see Reference 9 and Figure 3), it is possible to form a pressed strand measuring approximately 38 by 4 by 4 mm at pressures up to 150,000 psi. With this mold, sample strands of TNT for hot-plate pyrolysis have been pressed remotely at 20,000 psi.

c. In addition to the planned hot-plate pyrolysis studies of explosives, information on surface decomposition can be obtained from linear-deflagration-rate data. Along these lines, pressed strands of TNT have been burned in a Crawford bomb at pressures up to 1500 psi. The data obtained to date are somewhat scattered (see Table 1). This scatter is probably due to the use of a "wrap-around" technique for positioning the timing fuse wires. It is believed that better data can be obtained by inserting the timing wires through holes drilled in the strand. As more reliable burning-rate data become available, an analysis of the burning-rate, pressure dependence will be made, utilizing the "thermal-layer" treatment of combustion (Reference 6).

3. Theoretical Analysis

A theoretical elaboration of the studies described above has been carried out (Reference 10) for conventional high explosives.* An expression for the linear thermal-surface-regression rate of conventional, detonating, heterogeneous explosives (surface-evaporation rate in these cases) was derived and is of the form

$$B = AT_s \exp(-\Delta H_e/RT_s) \exp(-P\Delta V^o/RT_s) \quad (2)$$

where A is a constant related to molecule-collision frequency, T_s is the particle-surface or detonation temperature (Chapman-Jouguet), ΔH_e is the normal heat of evaporation of the explosive, P is the detonation pressure, R is the gas constant, and ΔV^o is the standard specific volume of activation.

The kinetic constants in Equation (2) were estimated for several granular high explosives on the basis of the assumptions that follow.

a. The rate-controlling step in the evaporation process involves surface desorption with a negligible entropy of activation. This leads to "normal" values for the pre-exponential factor (AT_s).

b. The formation of the activated state involves a 10% extension of the equilibrium bond length, which is taken as the distance (L) between molecules in the crystalline phase. This leads to

$$\Delta V^o \simeq 0.1\, L^3 \simeq 0.1\ (aM/\rho N) \quad (3)$$

where a is a lattice constant (~ 0.71 for hexagonal packing

M is the molecular weight of the explosive

ρ is the density of the solid explosive

N is Avogadro's number

For the explosives whose heats of evaporation are unavailable, it was assumed that $\Delta H_e \simeq 48\, T_m$ (where T_m is the melting temperature

*This work has been done in connection with Contract NOrd 17881.

in $^{\circ}K$), which is somewhat analagous to Trouton's rule. This empirical approximation has been tested with good results by Schultz and Dekker (Reference 11) for a large number of ionic solids which do not dissociate prior to evaporation. Table 2 lists calculated and experimental heats of vaporization (i.e., evaporation).

For the above assumptions Equation (2) becomes

$$B = 2.08 \times 10^{10} L T_s \exp\left[-\frac{8.5 \times 10^{-4} MP}{\rho T_s}\right] \exp\left[-\frac{\Delta H_e}{RT_s}\right] \text{ cm/sec} \qquad (4)$$

When P is in units of atmospheres and ρ is in gm/cm^3.

Table 3 gives the linear surface-regression rates for several high explosives, as calculated by Equation (4), and compares them with experimental data from Reference 12. These data suggest that the detonation reaction in granular explosives at nominal loading densities (i.e., ~ 1.2 gm/cm^3 or less) may be rate-controlled by an evaporation step.

At higher loading densities (i.e., higher detonation pressures), the surface-regression rate (B) appears to decrease (see Figure 4). This would lead to an increase in reaction time with increasing loading density, which is contrary to experiment (although the phenomenon of "dead pressing" of granular explosives may be related to this pressure effect). The same pressure effect is depicted in Figure 5 for reaction mechanisms other than surface evaporation. It is tentatively concluded that a true grain-burning detonation can probably occur only in low-energy explosives (e.g., NH_4NO_3 and NH_4ClO_4), or in conventional high explosives (TNT, PETN, etc.) that are packed to a relatively low charge density. Further work along these lines is being done.

B. BULK-COMPRESSION MECHANISM

1. Background

In contrast to the grain-burning theory of relatively recent origin, the concept of unimolecular, first-order, explosive, bulk decomposition stemming from shock compression has been discussed since the early history of detonation. The concept, for example, has long been the accepted mechanism of gaseous detonation.

There appear to be only two reasons why a grain-burning detonation theory need be considered at all. The first is that a particle-size influence on the nonideal detonation characteristics of heterogeneous explosives is almost always observed experimentally. The second reason is that at low charge densities the detonation shock is relatively weak and can (presumably) produce but little temperature rise through bulk compression of the explosive. On the other hand, this same weak shock can produce very high temperatures in the gas pockets and at grain-contact points in the explosive, which could give rise to fast surface burning.

Chaiken (Reference 13) has obtained quantitative evidence that a typical liquid high explosive (nitromethane) detonates through a unimolecular, first-order, bulk decomposition from shock compression. Detonation-reaction times were measured experimentally and related quantitatively to the unimolecular-decomposition kinetics of the compound. It was found that the reaction time could be expressed in the form

$$\tau = 1/k_{(bulk)} = A \exp (B/D^2) \qquad (5)$$

where A and B are constants relating to known parameters and D is the shock velocity. D can be related through the equation of state of the explosive to the shock temperature and pressure used in evaluating the bulk specific-rate constant, $k_{(bulk)}$.

Evidence that compressional bulk heating is a possible mechanism of propagation of detonation in conventional solid high explosives has also been obtained in investigations at Los Alamos (References 14 through 17). It was demonstrated that under suitable conditions of initiation, large single crystals of TNT, PETN, RDX, and tetryl can be made to detonate. The apparent lack of heterogeneity in single crystals thus seems to exclude grain burning in these cases. Moreover, the same general structure of the detonation-reaction zone observed by Chaiken for nitromethane has also been observed in a study conducted with single crystals of PETN (Reference 17).* The reaction-zone pressure profile of detonating solid (high-density) explosives, as obtained by the Los Alamos

*This point is discussed in greater detail in the appendix.

workers (References 14 and 15) also suggests a non-grain-burning mechanism for these explosives.

The general picture suggesting a grain-burning mechanism for the detonation of low-energy heterogeneous explosives and low-density, high-energy explosives, and a mechanism of unimolecular bulk decomposition from shock compression for high-density, high explosives is qualitatively consistent with most of the known experimental facts. However, much of this picture is still speculative, and further experimental studies to measure detonation velocities and reaction times under various conditions of shock initiation and charge design are being carried out in this investigation.

2. Reaction-Time Measurements

The measurement of detonation-reaction times employed here is based upon the techniques used by Cotter (Reference 18) and Chaiken (Reference 13). These techniques involve the use of explosive plane-wave generators to initiate detonation, and a high-speed, streak camera to follow the resulting luminescence. Observation and measurement of the reaction time of detonation initiation are based upon the assumption that the resulting detonation products in the Chapman-Jouguet plane radiate visible light, while the cooler region of the induction zone (which is essentially the reaction zone) is relatively nonluminous. This assumption is believed reasonable for completely degassed explosives (e.g., liquid explosives and granular explosives packed in a liquid medium) which detonate by a bulk-compression mechanism.

The degree of planarity of the initiating shock front is of great importance since significant errors in the interpretation of the streak-camera record are introduc when a curved shock front is present. Therefore, it was necessary to develop an explosive plane-wave generator which would yield an emerging shock wave having a high degree of planarity.

a. Test Apparatus and Procedure

An expendable test cell (see Figures 6 and 7) for observing and measuring reaction times in liquid explosives was designed and built. Modifications in the design will be incorporated to permit the cell to

be used with solid explosives. Nitromethane at 0°C was selected as a standard for the initial testing since it is homogeneous and optically clear, and previous results have been reported for its reaction time (References 12, 13, and 18). Optical clarity permits direct observation of the emission of light from the interior of the explosive during the entire detonation process.

The experimental approach to the cell design resulted in many modifications as the testing proceeded. Consider the nitromethane to be contained in an aluminum tube which has a 1.00-in. ID, a 0.012-in. wall thickness, and a 1.00-in. length; the resulting nitromethane volume is approximately 12.8 cc. The base of the explosive container rests on a thickness of Plexiglas,* which in turn is resting on the explosive plane-wave generator (see Figure 6). When the generator is detonated, a plane shock wave will be propagated through the plastic attenuator and into the liquid explosive. After a short delay, considered to be the reaction time, the chemical reaction will occur and will continue up through the explosive.

One of the most critical parts of the design was the attenuator-nitromethane interface. Plexiglas was chosen as the attenuator medium, due to its availability in suitable thicknesses and its optical clarity. It was also necessary to use a transparent Mylar film to act as a separating membrane, since Plexiglas is soluble in nitromethane. A 0.005-in. Mylar film adequately prevented the nitromethane from attacking the Plexiglas.

In order to eliminate possible optical distortion of the light observed by the camera slit, it was necessary to eliminate extraneous air bubbles and to make the top of the explosive container flat. A 1/4-in.-thick disk of Plexiglas surmounted the aluminum tube; a fill tube was placed off center through a hole in the disk so as not to interfere with the progress or observation of the detonation reaction. The fill tube was open to the atmosphere and acted as a reservoir maintaining constant initial pressure and volume within the cell with varying temperature.

A thin film of light machine oil coupled the Plexiglas to the Mylar film in order to eliminate the air space directly beneath the

*Rohm and Haas Company registered trade name for polymethyl methacrylate.

nitromethane. It was observed that any air space caused turbulence in the reaction front, which prevented accurate measurement of the reaction time. The Mylar was bonded to the aluminum tube with a Du Pont synthetic-rubber adhesive (No. 4684). This adhesive was selected because it was unaffected by nitromethane; it was used throughout the explosive cell. Several other adhesives were tested but were found to be unsuitable because of their solubility in nitromethane.

The explosive container is surrounded with a cardboard tube which has a 3-in. ID and a 1/4-in. wall thickness and is sealed to a Plexiglas plate which encloses the top of the air gap (Figure 6). The space between the explosive container and the cardboard tube was filled with an ice and water mixture about 1/2 hour before firing. The nitromethane was also refrigerated prior to testing. The ice and water bath kept the temperature of the whole device constant at $0^{\circ}C$, and equilibrium was reached well within the 1/2-hour period. The water that surrounded the explosive and occupied the largest portion of the cell volume also acted as a medium for suppressing extraneous light from the shock wave which would normally occur in air. The cell was positioned vertically in the firing chamber, and a front-surfaced mirror which was placed directly above the cell made a 45° angle with the line of sight of the camera. This allowed the camera slit to "look" down through the top of the explosive cell; the transparent cell permitted sharp focusing on the plane of the Mylar separating membrane on the bottom of the explosive container.

Air gaps were located at the under side of the Plexiglas baseplate (booster-pad, Plexiglas interface) and at the sides of the explosive container on the upper side of the baseplate. The air gaps in the cell acted as fiducial marks for measurement of the shock velocity and the reaction time. If air spaces were suitably located in the device, they would yield highly luminous zones as the shock passed through them. The air gaps contained the only air in the cell, since care was taken to eliminate air bubbles in the explosive and since the cell was surrounded by an ice and water bath. The distance between these gaps is the baseplate thickness, and the time required for the shock wave to travel that distance yields the initiating-shock velocity. The upper air gaps also indicate the time at which the shock enters the explosive column when a time

correction is applied for the plane shock to pass through the oil interface and the 0.005-in. thickness of Mylar film. The elapsed time between the appearance of these side gaps (due to shock compression) and the appearance of the luminescence from the detonation initiation is the reaction time.

A Beckman and Whitley Model 194, rotating-mirror, continuous-writing, streak camera with a 0.012-in. slit opening was utilized in the measurement of reaction times and shock velocities. It was used in conjunction with a Berkeley counter with a time base of 1 microsec to record turbine speed. The 0.012-in.-wide vertical slit on the camera allows a selected portion of the light from the event to enter the camera. The mirror can be rotated at speeds up to 5000 rps, which provides a maximum writing speed of 8 mm/microsec. A 35-mm strip of Kodak Tri-X film was used in the camera drum. The resulting continuous photographic record of the light intensity at the slit indicates position-time data, with time represented as film distance in the direction of mirror rotation, as shown in Figure 8. Time resolution is limited by the slit width, writing speed, mirror distortion, optical resolution of the camera-lens system, film sensitivity, and film shrinkage.

b. Results

(1) A series of 29 tests were conducted for the purpose of determining a conical explosive-plane-wave-generator composition having an optimum degree of planarity. A PBX (plastic-bonded explosive) exterior hollow cone was used in conjunction with a baratol interior solid cone which fits inside the PBX unit (see Figures 6 and 9). The results of a series of preliminary tests with baratol compositions varying from 33 to 100% in TNT indicated that a composition containing 74% of TNT and 26% of barium nitrate would give optimum planarity when used in conjunction with the PBX exterior cone.

Streak-camera measurements of the emerging shock front were made for eight plane-wave generators utilizing the optimum baratol composition. All parameters were held constant for the purpose of determining the range of planarity for the plane-wave generator units. The range was determined over an area representing the central 1-in.-dia circle and also for the area corresponding to the central 1.5-in. dia circle on the surface of the base of

of the baratol cone. The maximum deviation from planarity was determined from the film records, and the mean, median, and standard deviation of these maximum values were calculated. Figures 10a and 10b reproduce the film records obtained and list the deviations from planarity. The standard deviation (±0.017 microsec for the 1-in-dia area) was considered to be sufficiently small to allow accurate measurements of reaction time.

It was observed that by placing the detonator with its axis at a slight angle to the axis of the plane-wave-generator cones, a large deviation in planarity was introduced in the emerging shock wave. A detonator with a concave end, such as a No. 8, magnified the error introduced by misalignment of the detonator. This error was caused by the initiation of one side of the plane-wave generator in advance of the other side. The error was significantly reduced by using a mounting block for the detonator and by taking care in positioning the detonator.

(2) A series of 26 preliminary tests were performed in order to refine the techniques for measuring reaction times and shock velocities in nitromethane. A spectro-grade nitromethane was used which has a molecular weight of 61.04, a boiling point between 100 and 102°C, and a refractive index of 1.3825. The nitromethane was tested in the unsensitized state.

The above-mentioned plane-wave generators were utilized as initiating devices in conjunction with a booster pad, which increased the momentum and the velocity of the emerging shock wave.

The initial tests resulted in reaction times which were not resolved by the streak camera; this indicated that the nitromethane detonated within 0.01 microsec from the time the shock wave entered the nitromethane. Film Record No. 682 in Figure 11 provides an example of an unresolved reaction time. In such cases, the initiating shock velocity was greater than 6200 m/sec, which is approximately the steady-state detonation velocity in nitromethane.

The remaining film records shown in Figure 11 depict a series of resolved reaction times for detonation initiation in

nitromethane. The still photographs are shown to the right of the streak records. Time events are progressing with increasing time from right to left on the film. The nitromethane was contained in a 1.00-in. aluminum tube in all tests except No. 771, in which a 1.00-in. glass tube was employed.

A 0.120-in. Plexiglas baseplate surmounted by a 0.254-in. baseplate was used when Record No. 765 was obtained; this explains the two vertical light flashes shown in the film. The average shock velocity through the first baseplate was 7870 m/sec, and the average shock velocity through the second was 5750 m/sec. A 2-in.-dia tetryl booster pad was used in conjunction with the plane-wave generator. The horizontal streak which runs through the length of the detonation zone is due to the optical interference produced by the glass fill tube which had been positioned too close to the slit of the camera; this can be observed in the still photograph. The light flashes on each side of the explosive container indicate, after a suitable correction for the Mylar film, the instant at which the shock wave entered the explosive; these flashes are produced by the 0.010-in. air gap on the top of the upper baseplate. On the film, the reaction time is measured horizontally from the right-hand side of these light flashes to the initial point of detonation (i.e., the first appearance of luminescence).

Test No. 772 employed a 0.269-in. Plexiglas baseplate, without a booster pad. Test No. 776 was similar to No. 765; a tetryl booster pad was utilized, and the thicknesses of the two Plexiglas baseplates were 0.119 and 0.269 in.

Film Record No. 771 (nitromethane in glass-tube confinement) shows evidence of three zones of luminosity in the detonation-initiation front. This apparent-multiple-zone structure was also noted in the previous investigations by Cotter (Reference 18) and Chaiken (Reference 13).* It was considered to be the result of a "super-velocity" reaction wave moving behind the initiating shock front (Reference 13). A detailed description of this possible phenomonon is given in the appendix.

*A glass-tube confinement was employed in Chaiken's previous work. At present, the nature of the nitromethane confinement in Cotter's studies is not known.

It is interesting to note that the luminosity from the reaction front as depicted in the other film records (Nos. 765, 772, and 776; nitromethane in aluminum-tube confinement) apparently only shows a two-zone structure. This apparent discrepancy between the results obtained with glass and aluminum containers is being investigated further.

The experimental reaction-time data acquired to date, which are thought to be reliable, are presented in Table 4 and plotted in Figure 12. The reaction times have been corrected for the thickness of the oil and Mylar films in the cell. In general, the curve in Figure 12 approaches that given in Reference 13 except in the region of low shock velocity (5000 to 5300 m/sec). However, further data will be required before detailed comparison and analysis of the results can be made. It is expected that these data will be obtained in the near future.

3. Theoretical Calculations

Theoretical calculations of the expected variation of detonation-reaction time with ambient temperature in nitromethane have been carried out. Utilizing the theoretical and experimental results described in Reference 13, the relationship between reaction time (τ , sec) and initial charge temperature (t, ^{o}C) or density ($\rho_o = 1/V_o$, gm/cm^3) for an initiating shock velocity of 5700 m/sec can be expressed as

$$\ln \tau = \frac{1.228\ (V_o - 0.46) + 2.84\ V_o^2}{(V_o - 0.46)^2} - 32.982 \qquad (6)$$

and

$$\rho_o = 1/V_o = 1.159 - 1.33 \times 10^{-3} t \quad \text{gm/cm}^3$$

Figure 13 depicts a plot of $\ln \tau$ vs t using the above expressions. It is interesting to note that below $\sim 30^{o}$C, the values for τ fall within the realm of observation by the streak-camera techniques described in Section III,B,2. Experimental verification of the curve in Figure 13 will be attempted. Such verification would lend added support to the applicability of a first-order, bulk-compression, detonation mechanism in nitromethane.

It is planned to undertake similar theoretical developments for high-density solid explosives.

C. DETONATION-VELOCITY MEASUREMENTS

As discussed in Section III,B,1, it is believed that detonation can proceed by a grain-burning and/or a bulk-compression mechanism. It was thought that a comparison of the shock sensitivity and detonation velocity of cylindrical charges of granular explosives with different void fillers (air, propane, water, nitromethane, etc.) would afford information concerning the regions of applicability of these mechanisms. Toward this end, the detonation velocities of granular TNT packed in air, water, and nitromethane have been measured with a Beckman and Whitley Model 194 streak camera. An error analysis of the present streak-camera techniques indicates that detonation-velocity measurements of detonating, 6-in.-long, cylindrical, explosive charges are good to within $\pm 1.5\%$.

Figure 14 shows a sample series of streak-camera records obtained utilizing a glass-tube charge container (6-in. length, 0.97-in. ID, and 0.05-in. wall thickness) and a Composition C-4 booster pad (1-7/8 in. in dia by 2 in. long). It is of interest to note the decreased luminosity of detonating nitromethane relative to TNT (compare Records No. 612 and 608). Record No. 603 had a camera writing speed of 0.8 mm/microsec, while the remaining records had a writing speed of 1.6 mm/microsec; this would explain the increase in the luminosity of Record No. 603 relative to that of Record No. 612.

The averaged velocity data of 33 shots are listed in Table 5 for TNT with various void fillers. It is interesting to note that TNT and water detonates with a velocity comparable to TNT and air, while TNT and nitromethane detonates with a velocity comparable to that of nitromethane alone. These studies will be continued.

IV. FUTURE WORK

The program of study discussed above will be continued as part of the work carried out under Contract AF 49(638)-851. Attempts will be made to

A. Measure the linear pyrolysis rate of TNT and other high explosives

B. Obtain linear-burning-rate data on pressed strands of TNT and other solid explosives

C. Measure the reaction time of detonation in nitromethane and other explosives

D. Determine the detonation characteristics of granular explosives in various fillers

E. Develop a consistent theory for the mechanisms of deflagration and detonation in condensed explosives.

V. PROJECT PERSONNEL

The project personnel who were engaged in whole or in part in carrying out the investigations described in this report are listed below.

A. CHEMICAL DIVISION

R. F. Chaiken, Technical Specialist

I. Geller, Research Chemist

P. A. Kees, Laboratory Technician

B. ORDNANCE DIVISION

W. H. Andersen, Technical Specialist

J. R. Cullinan, Ordnance Technician

P. A. O'Donovan, Research Engineer

K. J. Schneider, Research Engineer.

REFERENCES (TEXT)

1. H. Eyring, R. E. Powell, G. H. Duffey, and R. B. Parlin, Chem. Rev., 45, 69 (1959).

2. F. B. Bowden and A. D. Yoffe, Initiation and Growth of Explosion in Liquids and Solids, Cambridge, University Press, 1952.

3. W. H. Andersen and R. F. Chaiken, "Application of Surface Decomposition Kinetics to Detonation of Ammonium Nitrate," ARS Journal, 29, 49 (1959).

4. W. H. Andersen and R. F. Chaiken, On the Detonability of Solid Composite Propellants, Part I, Aerojet-General Technical Memorandum No. 809, January 1959.

5. W. H. Andersen, K. W. Bills, E. Mishuck, G. Moe, and R. D. Schultz, "A Model Describing Combustion of Solid Composite Propellants Containing Ammonium Nitrate," Combustion and Flame, 3, 312 (1959).

6. R. F. Chaiken, "A Thermal Layer Mechanism of Combustion of Solid Composite Propellants: Application to Ammonium Nitrate Propellants," Combustion and Flame, 3, 285 (1959).

7. M. K. Barsh, W. H. Andersen, K. W. Bills, G. Moe, and R. D. Schultz, "An Improved Instrument for the Measurement of Linear Pyrolysis Rates," Rev. Sci. Instruments, 29, 392 (1958).

8. R. F. Chaiken and D. K. Van de Mark, "Thermocouple Junction for a Hot-Plate Linear Pyrolysis Apparatus," Rev. Sci. Instruments, 30, 375 (1959).

9. R. Friedman, R. G. Nugent, K. E. Rumbel, and A. C. Scurlock, "Deflagration of Ammonium Perchlorate," Sixth Symposium (International) on Combustion, New York, Reinhold, 1957, pp. 612-618.

10. W. H. Andersen, Investigations for Improving the Usefulness of High Explosives at Elevated Temperatures, Aerojet-General Report 1657, September 1959.

11. R. D. Schultz and A. O. Dekker, The Absolute Thermal Decomposition Rates of Solids. Part III - The Vacuum Sublimation Rate of Ionic Crystals, OSR-TN-55-138 (Aerojet-General TN-7), July 1955.

12. M. A. Cook, The Science of High Explosives, New York, Reinhold, 1958.

13. R. F. Chaiken, "The Kinetic Theory of Detonation of High Explosives," M.S. Thesis, Polytechnic Institute of Brooklyn, 1958.

14. R. E. Duff and E. Houston, J. Chem. Phys., 23, 1268 (1955).

REFERENCES (TEXT) (cont.)

15. W. E. Deal, J. Chem. Phys., 27, 796 (1957).

16. A. W. Campbell, M. E. Malin, and T. E. Holland, Second ONR Symposium on Detonations, Washington, D.C., Office of Naval Research, February 1955.

17. T. E. Holland, A. W. Campbell, and M. E. Malin, J. Applied Phys., 28, Y217 (1957).

18. T. P. Cotter, "The Structure of Detonation in Some Liquid Explosives," Ph.D. Dissertation, Cornell University, 1953.

TABLE 1

CRAWFORD-BOMB BURNING-RATE DATA FOR TNT (RESTRICTED STRANDS)

Pressure atm	Number of Strands	Burning Rate cm/sec	Experimental Standard Deviation cm/sec
1	2	0.18*	±0.00
34	5	0.29	±0.13
68	4	0.79	±0.63
102	3	3.49	±2.35

*Strand sliver remained on both strands, indicating non-cigarette-type burning.

TABLE 2

HEATS OF VAPORIZATION FOR SEVERAL EXPLOSIVES

Explosive	T_m, °K	Heat of Vaporization, cal/mole	
		Calculated	Experimental
TNT	353	16,940	17,600
Nitroglycerin	286	13,730	13,870
PETN	414	19,880	17,840
Tetryl	403	19,340	--
Picric acid	395	18,960	--
RDX	477	22,900	--

TABLE 3

ESTIMATES OF LINEAR RATE OF SURFACE REGRESSION DURING DETONATION OF GRANULAR EXPLOSIVES

Explosive	Linear Rate of Surface Regression, cm/sec			
	Calculated by Equation (4)	Curved-Front Theory	Nozzle Theory	Geometric Theory
TNT ($3700^{\circ}K$; 60,000 atm)				
$\rho_o = 1.0$ gm/cm^3	6.26×10^4	1×10^5	3.85×10^4	3.85×10^3
PETN ($5350^{\circ}K$; 80,700 atm)				
$\rho_o = 0.95$ gm/cm^3	1.68×10^5	3.33×10^5	1.11×10^5	1.25×10^4
RDX ($5250^{\circ}K$; 114,000 atm)				
$\rho_o = 1.2$ gm/cm^3	1.04×10^5	2.5×10^5	1×10^5	1×10^4
Tetryl ($4200^{\circ}K$; 71,200 atm)				
$\rho_o = 0.95$ gm/cm^3	5.16×10^4	--	3.33×10^4	5.88×10^3

TABLE 4

VARIATION OF REACTION TIMES WITH INITIATING-SHOCK VELOCITIES FOR NITROMETHANE

(All Tests Run at 0°C with Aluminum Confinement)

Streak-Camera Record No.	Initiating Shock Velocity m/sec	Corrected Reaction Time τ, microsec
737	5225	0.424
738	5626	0.175
743	5126	0.519
744	5660	0.171
759	5526	0.192
765	5750	0.078
767	6193	0.00
772	5895	0.165
773	5979	0.171
775	5098	0.335
776	6056	0.016

TABLE 5

DETONATION VELOCITIES OF GRANULAR TNT PACKED IN VARIOUS MEDIA*

Initial TNT Packing Density gm/cm³	Fluid Medium	Detonation Velocity m/sec
0.73	Air	4140
0.87	Air	4400
0.73	Water	3880
0.73**	Nitromethane	6300
0	Nitromethane	6150

*All tests were performed under ambient conditions.

**Approximately 30% of the TNT dissolved in the fluid medium prior to detonation.

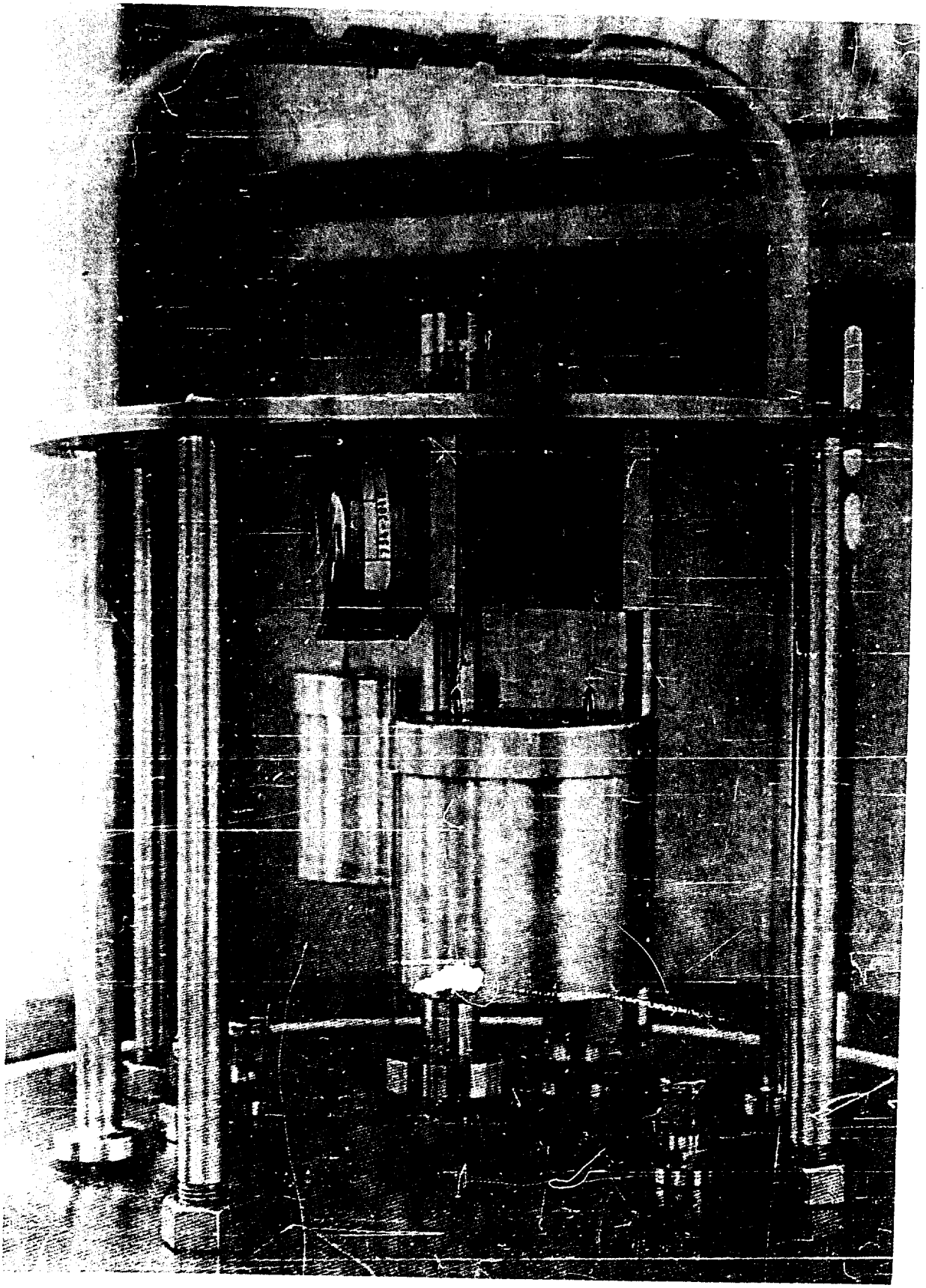

Hot-Plate-Pyrolysis Bomb - Interior View

Figure 1

Hot-Plate-Pyrolysis Bomb

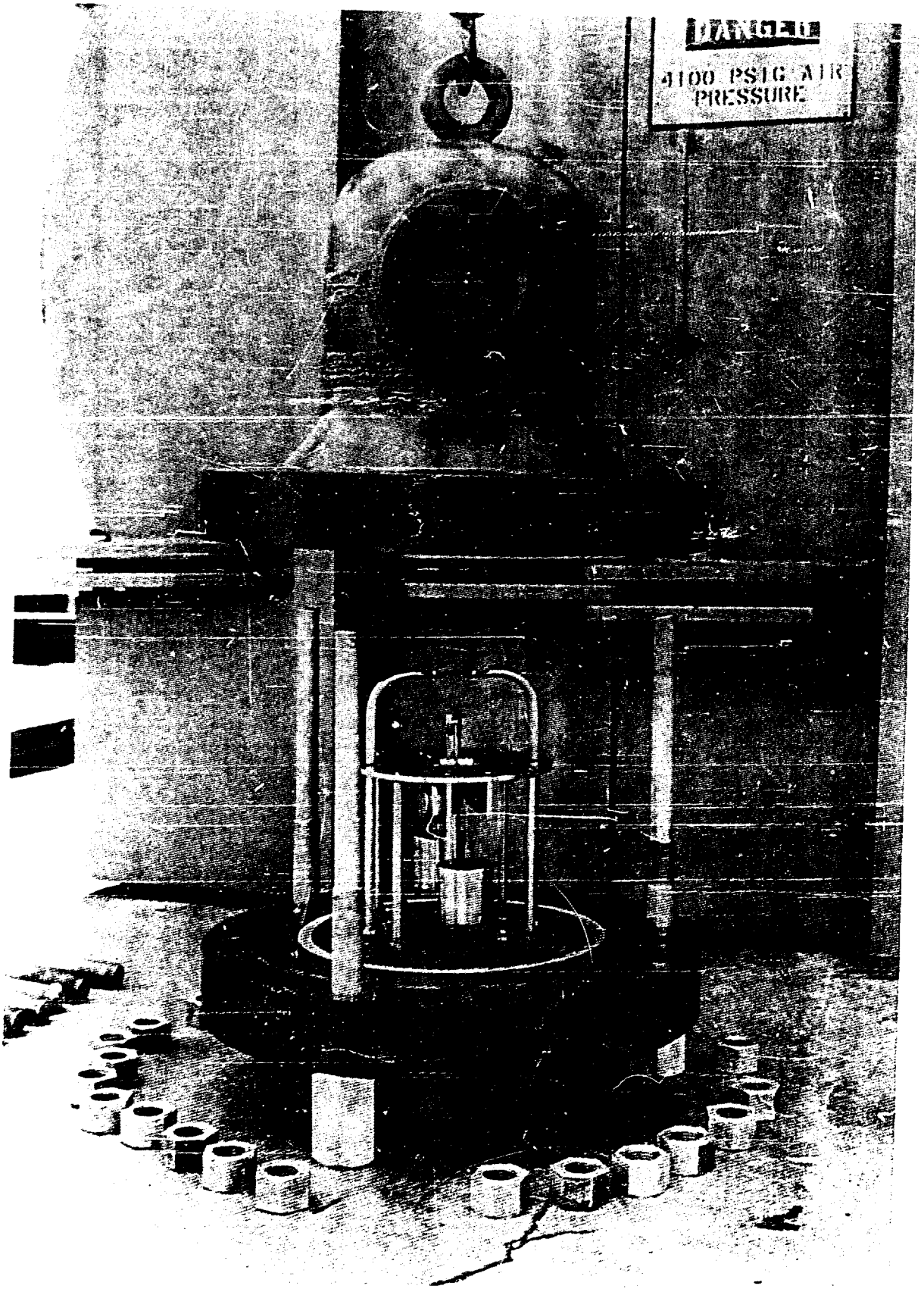

Hot-Plate-Pyrolysis Bomb - Entire View

Figure 2

Components of Strand Mold
(Atlantic Research Corporation Photo)

Figure 3

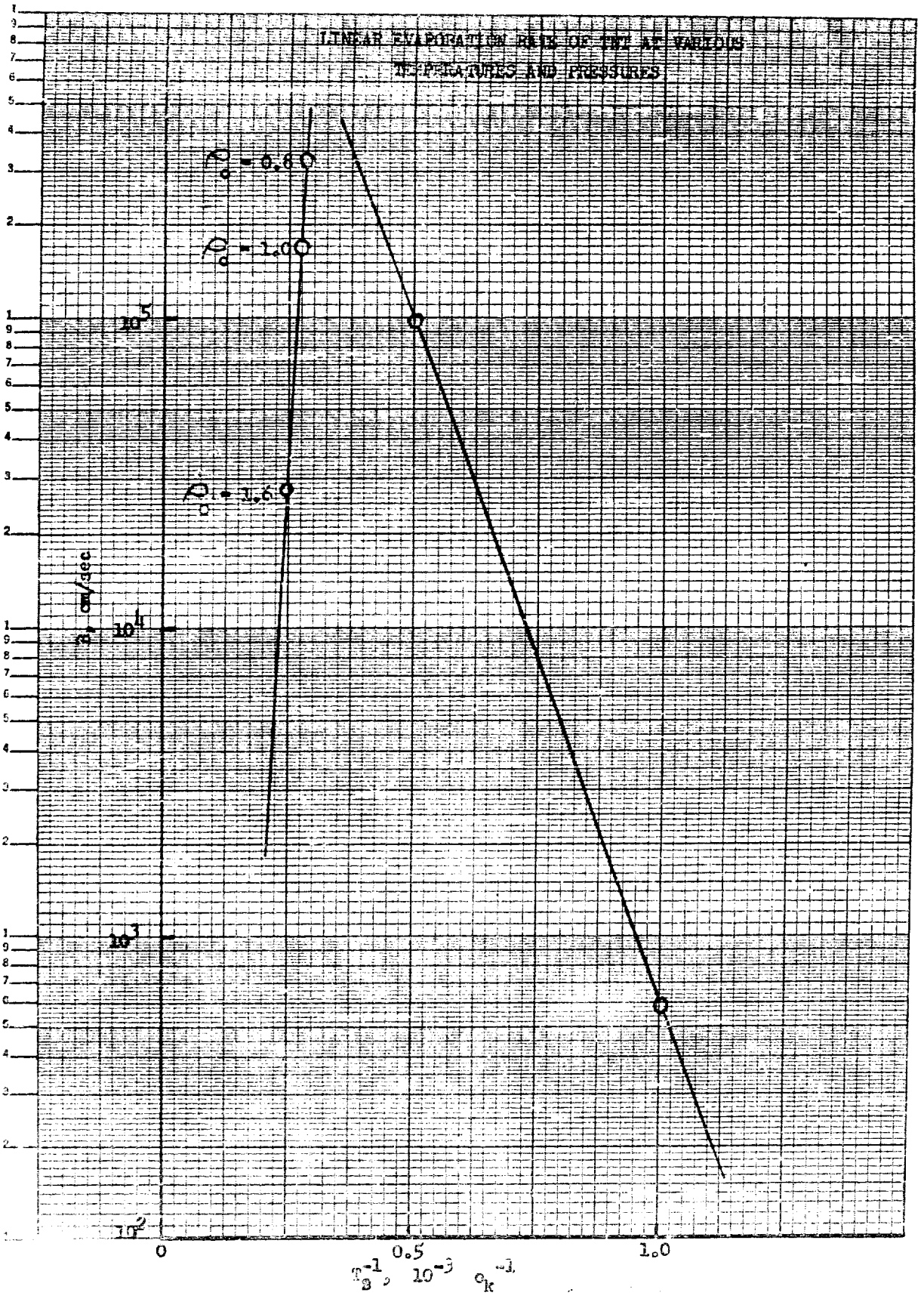

Figure 4

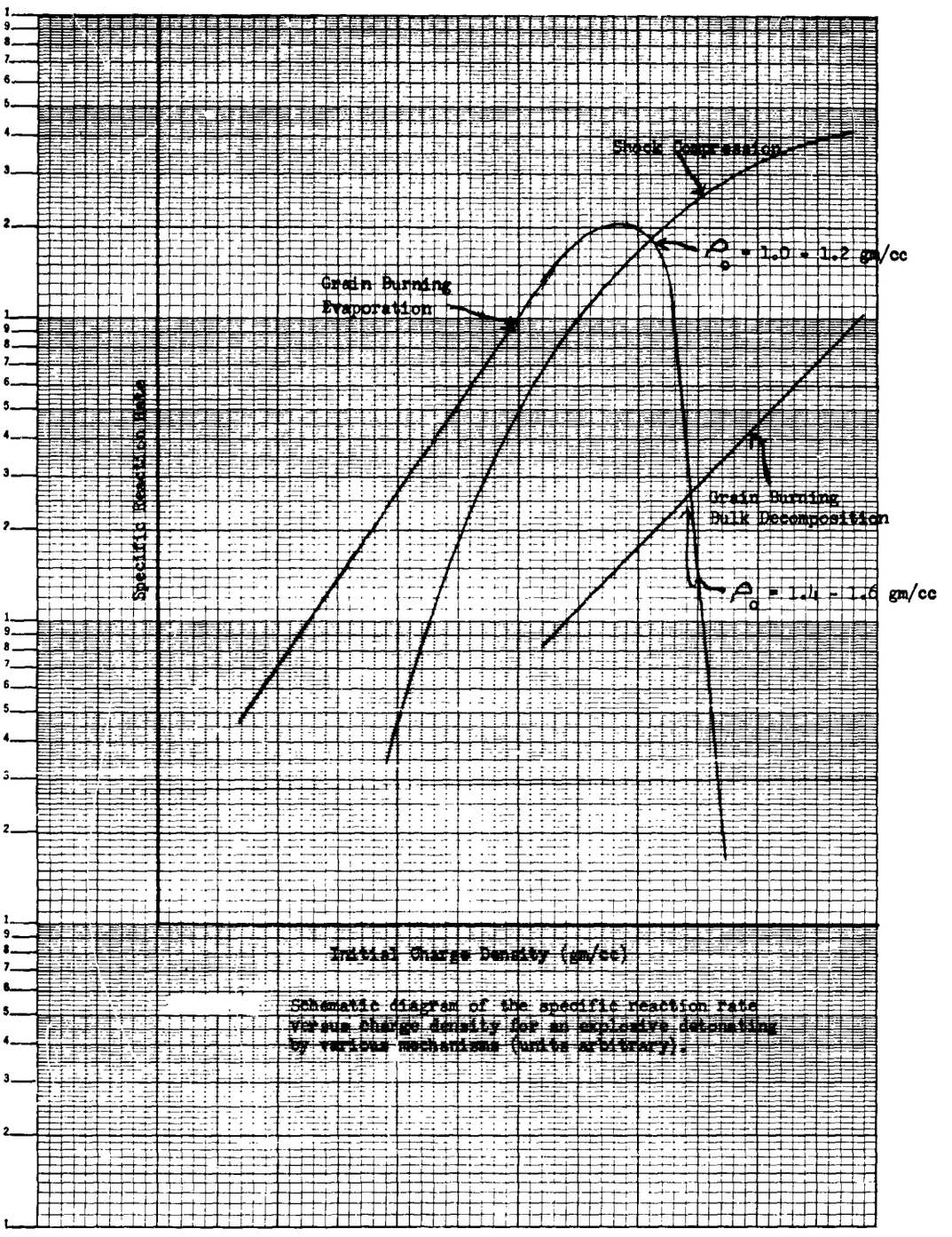

Schematic diagram of the specific reaction rate versus charge density for an explosive detonating by various mechanisms (units arbitrary).

Figure 5

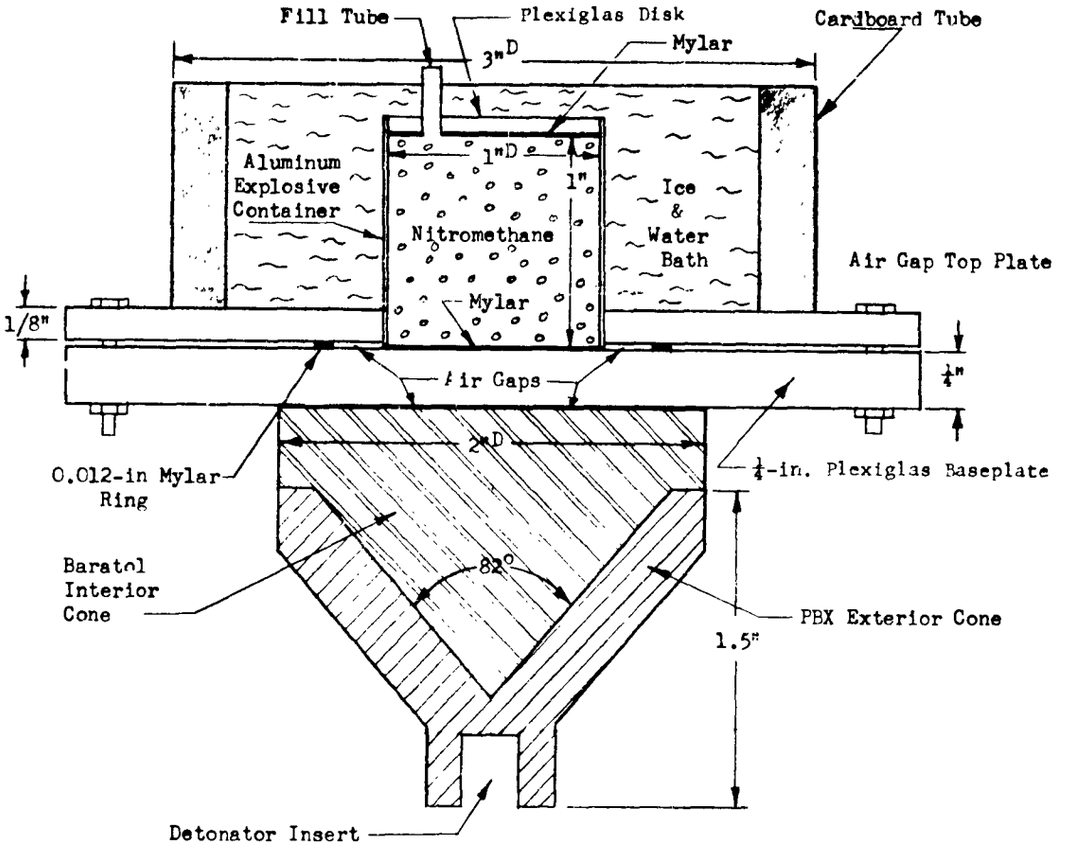

EXPERIMENTAL ARRANGEMENT OF

TEST CELL AND EXPLOSIVE CHARGE

Figure 6

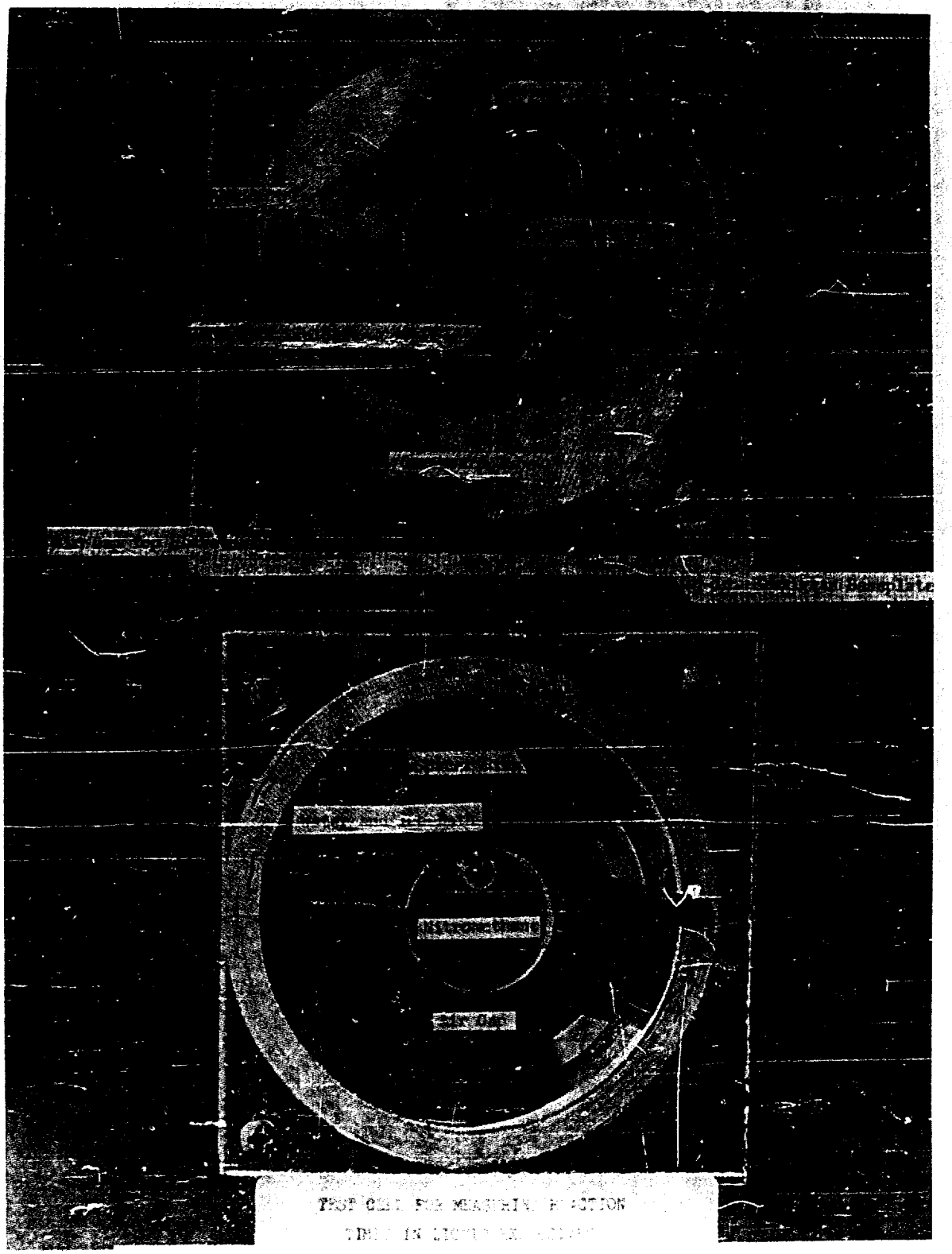

Best Available Copy

Figure 7

SIDE VIEW OF EXPLOSIVE TEST CELL SYSTEM
AND STREAK CAMERA RECORD

Figure 6

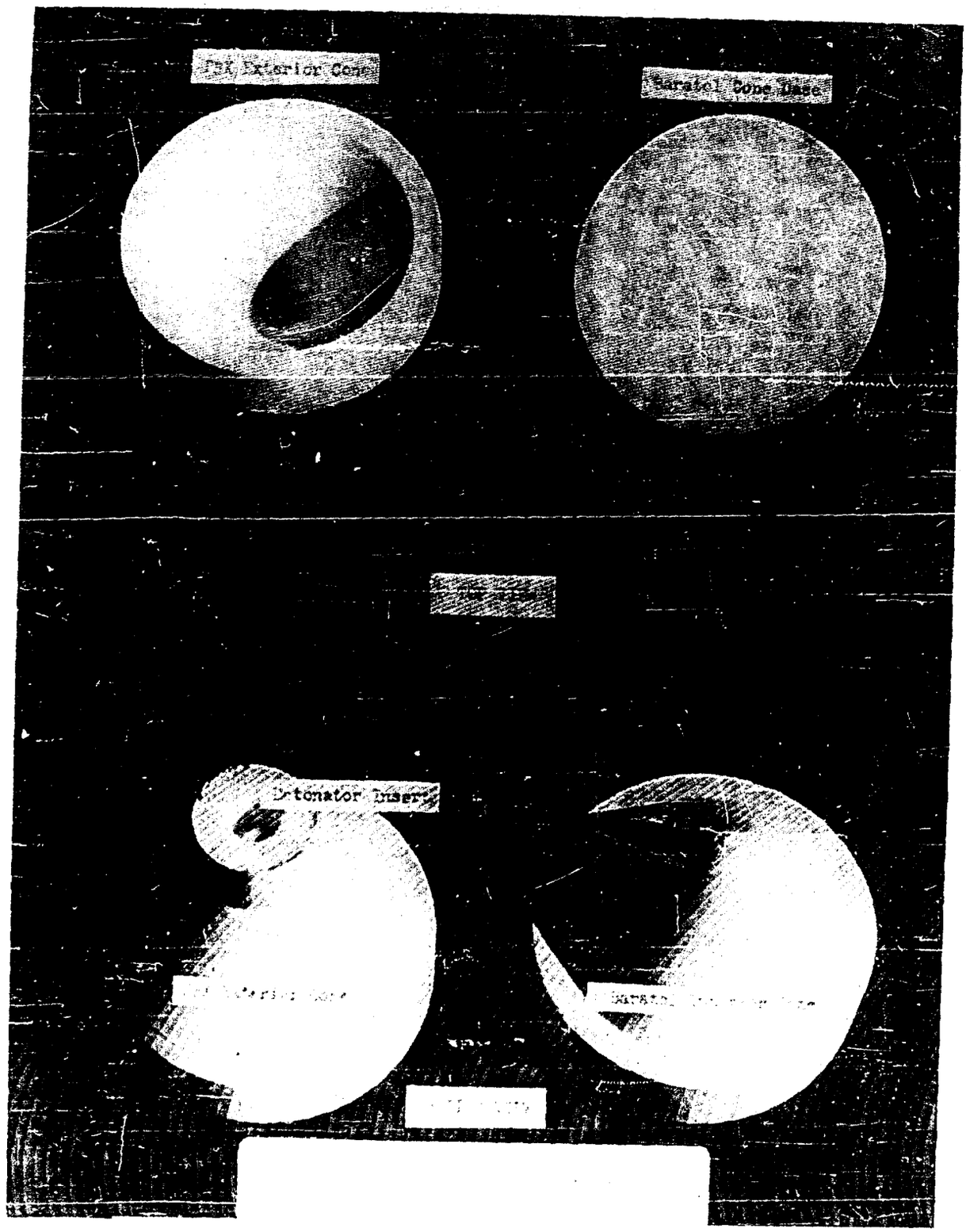

Figure

PBA - [illegible] REGENERATOR SERIES
7[illegible] TEST [illegible]
STREAK CAMERA STUDY

No. 710
Camera Speed = 5[illegible]
Writing Speed = 3.[illegible] mm/μ s

Maximum Deviation	
1st D	1st D
0.24 μ s	0.12 μ s

No. 711
Camera Speed = [illegible]
Writing Speed = 3.3 mm/ s

Maximum Deviation	
1st D	1st D
.[illegible] s	0.0[illegible] μ s

No. 712
Camera Speed = [illegible]
Writing Speed = 3.22 mm/ s

Maximum Deviation	
1st D	1st D
.[illegible] s	0.02 μ s

No. 33
Camera Speed = [illegible]
Writing Speed = [illegible] mm/ s

Maximum Deviation	
1st D	1st D
[illegible]	[illegible] s

Figure 10a

re 9

PBX - BARATOL PLANE-WAVE GENERATOR SERIES
74% TNT BARATOL
STREAK CAMERA STUDY

No. 714
Camera Speed = 5232 RPS
Writing Speed = 8.37 mm/μs

Maximum Deviation	
1"D	1½"D
0.04 μs	0.10 μs

No. 716
Camera Speed = 5119 RPS
Writing Speed = 8.19 mm/μs

Maximum Deviation	
1"D	1½"D
0.07 μs	0.13 μs

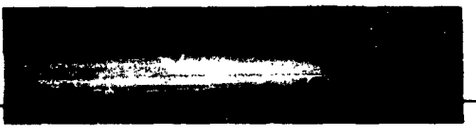

No. 717
Camera Speed = 5061 RPS
Writing Speed = 8.10 mm/μs

Maximum Deviation	
1"D	1½"D
0.01 μs	0.04 μs

Maximum Deviation From Planarity

	1"D	1½"D
Mean	0.037 s	0.072 s
Median	0.040 s	0.060 s
Std. Deviation	±0.017 s	±0.041 s

Figure 10b

[illegible] OF DETONATION

[illegible] Detailed Study of Minimum Charge

Reaction Times

No. 682

Camera Speed-1002 RPS Writing Speed 1.71 mm/μs

No. 765

Camera Speed-2501 RPS Writing Speed-4.00 mm/μs
Shock Velocity-5750m/s Reaction Time-0.076 μs

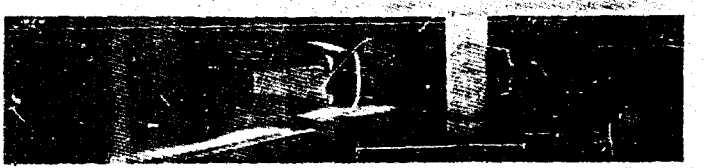

No. 771

Camera Speed-2515 RPS Writing Speed-4.02 mm/μs
Shock Velocity-5700m/s Reaction Time-(1)0.162 μs
(2)0.302 μs

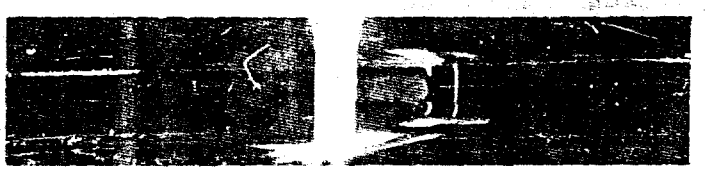

No. 772

Camera Speed-2509 RPS Writing Speed-4.01 mm/μs
Shock Velocity-5765m/s Reaction Time-0.165 μs

No. 770

[illegible] Writing Speed-4.02 mm/μs
[illegible] Reaction Time-[illegible] μs

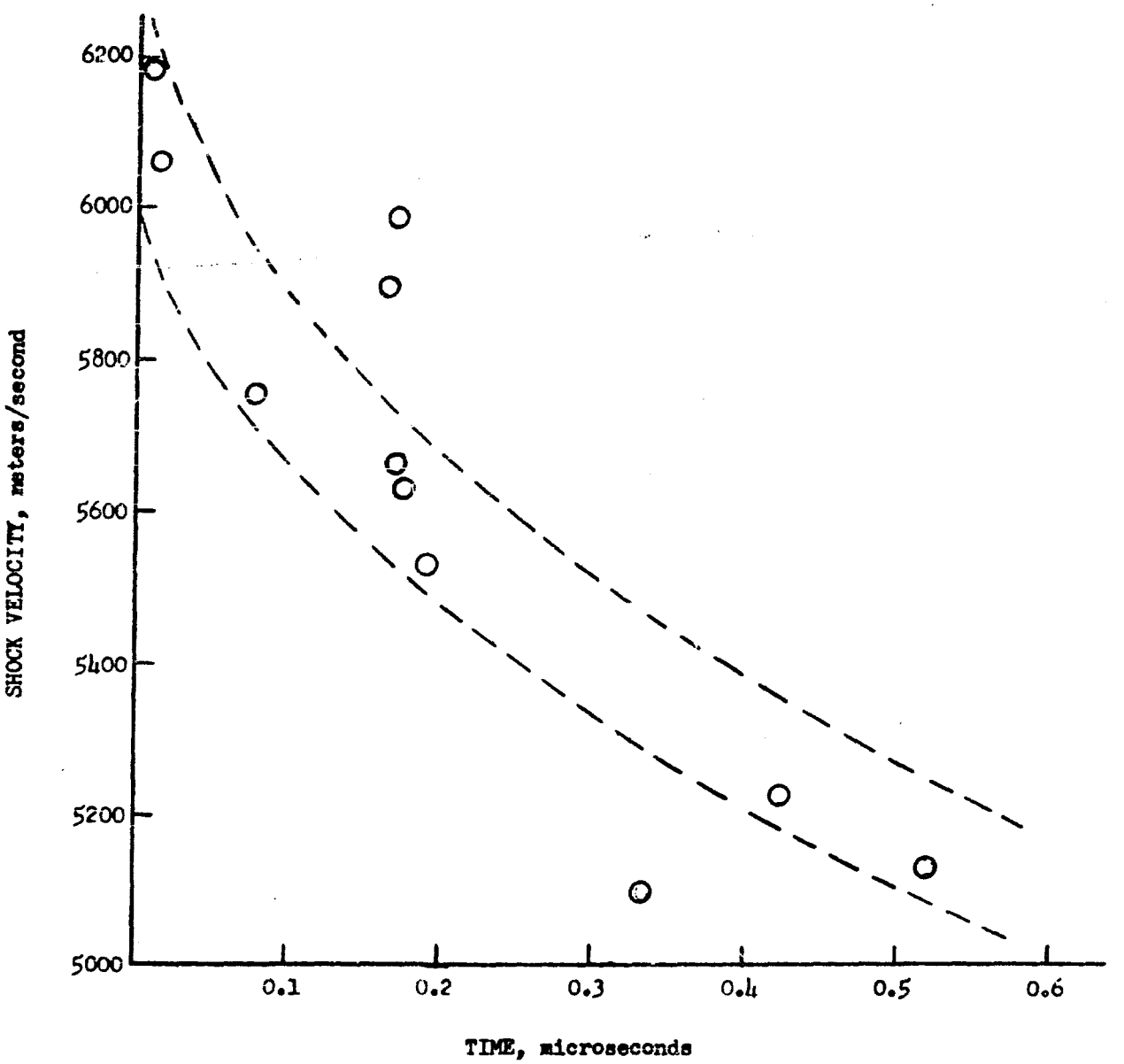

REACTION TIMES OF NITROMETHANE WITH VARYING INITIATING-SHOCK STRENGTHS

All tests run at 0°C with aluminum confinement

Figure 12

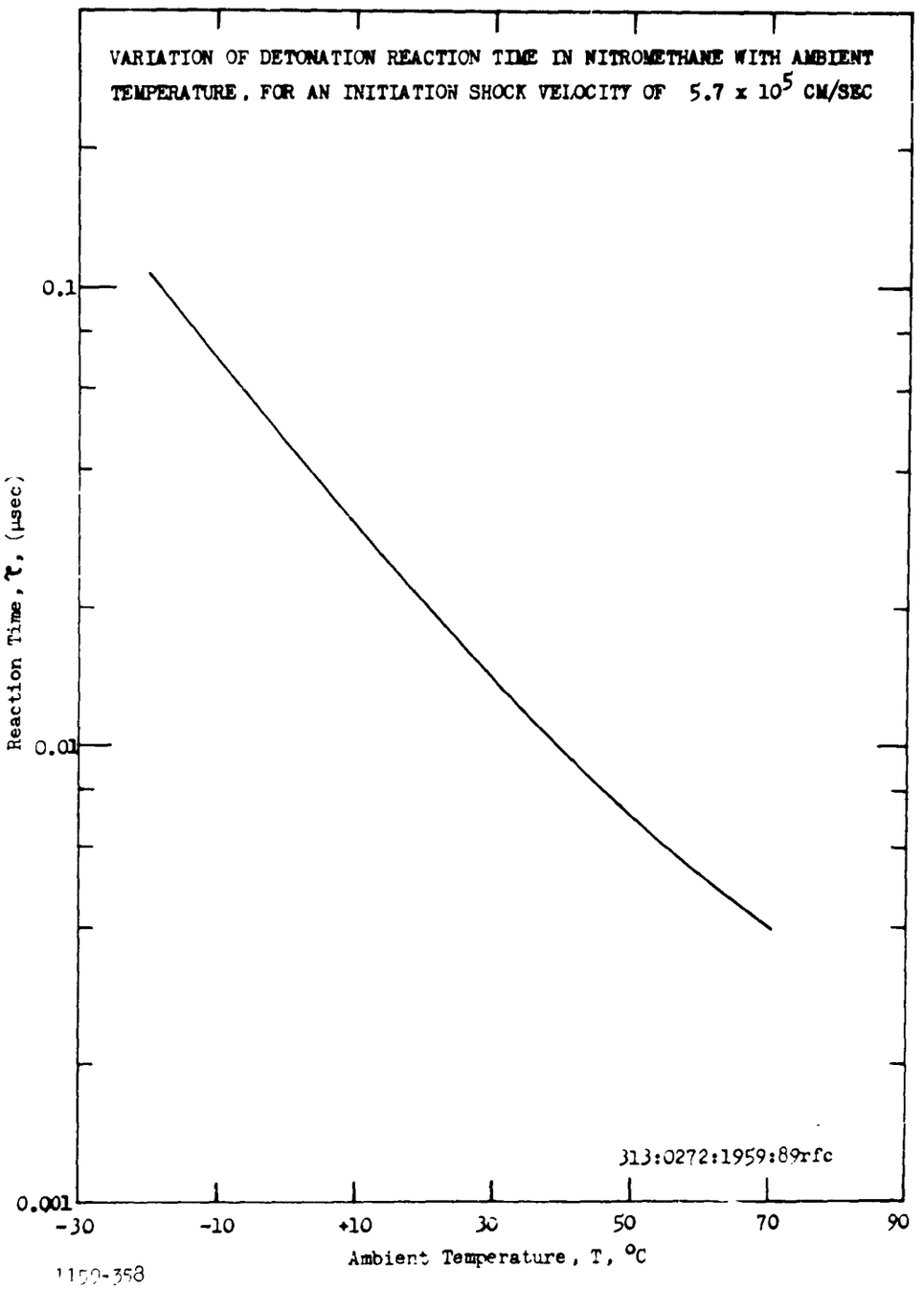
VARIATION OF DETONATION REACTION TIME IN NITROMETHANE WITH AMBIENT TEMPERATURE, FOR AN INITIATION SHOCK VELOCITY OF 5.7 x 10^5 CM/SEC
Reaction Time, τ, (μsec)
0.1
0.01
0.001
313:0272:1959:89rfc
-30
-10
+10
30
50
70
90
Ambient Temperature, T, °C
1159-358

Figure 13

Velocity Studies.

No. 603

Aver. Vel. = 5903 m/s

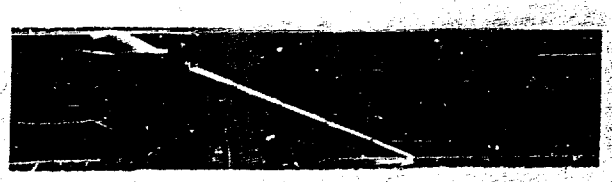

No. 608

Aver. Vel. = 4451 m/s

No. 613

Aver. Vel. = [illegible] m/s

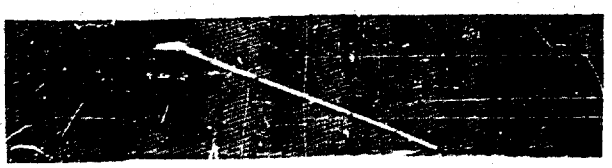

No. 613

Figure 14

APPENDIX

COMMENTS ON HYPERVELOCITY-WAVE PHENOMENA IN CONDENSED EXPLOSIVES*

The direct observation of hypervelocity-wave phenomena during detonation initiation by strong shocks in single crystals of PETN and liquid nitromethane have been reported by Holland, Campbell, and Malin (Reference 1) and by Cook, Pack, and Gey (Reference 2), respectively.

Holland, et al. noted, by means of streak-camera photography of shock-impacted large crystals of PETN, that the growth of detonation toward steady-state conditions apparently proceeded in several stages. First, a relatively low velocity wave front (5.56 mm/microsec) appeared and abruptly changed to a very high velocity compression wave ($\sim$ 10.45 mm/microsec). Within $\sim$0.5 microsec, the high-velocity front changed to an apparent steady-state detonation (8.28 mm/microsec) which consumed the crystal. No explanation was offered as to the nature of these events.

From similar space-time, high-speed-camera studies of the shock initiation to detonation in nitromethane, Cook and his co-workers observed a "flash-across" phenomenon in which an apparent wave of luminescence originated in the explosive behind the initial compression front, and propagated at a reported velocity of $\sim$35 mm/microsec to overtake the initial compression front. This "flash-across" phenomenon was interpreted as a heat-transfer wave caused by a sudden increase in the thermal conductivity of the shock-compressed nitromethane. The phenomenon was taken as a direct observation of the "heat pulse" which Cook, Keyes, and Filler had predicted (Reference 3).

---

*Prepared for submission to the Journal of Chemical Physics by R. F. Chaiken on the basis of work supported by ARPA under Contract Nonr 2804(00) monitored by the Office of Naval Research.

Several years prior to the studies by Cook, Pack, and Gey (subsequently referred to as CPG), the author carried out a streak-camera study of shock initiation to detonation in nitromethane (Reference 4). At that time, evidence was found to indicate the existence of a hypervelocity wave moving behind the initiating shock front. It was suggested that the detonation-reaction wave originated behind the initial compression front and traveled at a "super-velocity" in the compressed explosive to overtake the initiating shock front.

The author believes that this detonation-initiation process could be an alternative explanation for the "flash-across" phenomenon observed by CPG, and that it also offers an explanation for the velocity steps in PETN which were observed by Holland, et al.

Figure 1 is a space-time plot of the wave phenomena occuring during detonation initiation in nitromethane, based upon the author's studies (Reference 4). Referring, for the time being, only to Time Zones I and II, D_i is the initiating-shock velocity (i.e., the velocity of the shock wave entering the explosive from an external source); D' is the hypervelocity-wave velocity; u is the velocity imparted to the explosive by the initiating shock wave; τ is the time lag between compression and luminescence from any element of fluid at an initial distance S from the point where the initiating shock front enters the explosive; and τ_o refers to the observed time lag for the fluid element at S = 0.

In Time Zones I and II, the CPG observations apparently coincide with the author's, except for the magnitude and interpretation of τ_o and D'.

Assuming that D_i and D' are independent of S (i.e., negligible attentuation of the wave fronts in the explosive), it is possible to express τ as a linear function of S.

From Figure 1, the following relations hold:

$$S = u(\tau_o - \tau) + S' \qquad (1)$$

and

$$S' = D'\Delta t = \Delta S_1 + u\Delta t \qquad (2)$$

From the Rankine-Hugoniot (R-H) relationships for one-dimensional steady-state shock propagation,

$$\Delta S_1 = (V/V_o)S \tag{3}$$

where V/V_o is the ratio of specific volumes across the shock front (with subscript o referring to the initial state).

Equations (1) through (3) can be rearranged to yield

$$T = T_o - (S/u)\left[D'(1 - V/V_o) - u\right] \Big/ \left[D' - u\right] \tag{4}$$

From the R-H equations, $u/D_i = 1 - V/V_o$; therefore, Equation (4) becomes

$$T = T_o - \left[(D'/D_i - 1) \Big/ (D' - u)\right] S \tag{5}$$

Equation (5) is the same as the CPG experimental equation, i.e.,

$$T = T_o - a'S \tag{6}$$

where a' is a positive constant having the measured value of $\sim$1.7 microsec/cm. For this value of a', and taking D' = 35 mm/microsec and $u = 0.45\ D_i$, the initiating-shock velocity in the CPG experiments turns out to be $\sim$5.3 mm/microsec. This value of D_i falls within the range of values studied by the author.

In Figure 2, a plot of a' vs D' is given for D_i = 5.3 mm/microsec and u = 2.4 mm/microsec. Superimposed upon this curve are the results of the two studies. It is seen that the CPG values for a' and D' differ by the respective factors of $\sim$0.25 and $\sim$3 from the author's values. However, it is easily seen that in the vicinity of a' = 1.7 microsec/cm, it would be very difficult to calculate an accurate value for D' on the basis of an experimentally measured a'. This might be a reason for the discrepancy in the two sets of results.

It is interesting to note that if it is assumed that the chemical-reaction wave resulting in D' has a velocity comparable to a steady-state detonation velocity (D_s) at the shock density ($\rho = 1/V$), an estimate of D' might be obtained from extrapolated $D_s(\rho)$ data. From the work of Campbell, Malin, and Holland on the detonation velocity of nitromethane as a function of initial temperature (Reference 5), the following expression for $D_s(\rho)$ can be obtained:

$$D_s = 2.78 \times 10^3 \rho + 3110 \text{ m/sec} \quad (7)$$

Estimating that $\rho \simeq 2.1$ gm/cm^3 for $D_i \simeq 5.3$ mm/microsec yields a steady-state detonation velocity of 8.86 mm/microsec. Since this reaction wave would be traveling in a moving medium,

$$D' = D_s + u \simeq 11.5 \text{ mm/microsec} \quad (8)$$

which is consistent with the author's value.

The formation of a propagated "super-velocity" reaction wave is also consistent with an adiabatic-reaction model in which the chemical-reaction rate exhibits an apparent induction time (τ_o). After τ_o seconds pass, the molecules of explosive which were first compressed by the initiating shock front suddenly decompose. The rapid release of energy propagates a high-pressure reaction wave moving with velocity of $D' > D_i$ behind the initiating shock front. This "super-velocity" reaction wave overtakes the initiating shock front and passes into the unshocked region. The detonation reaction in the nitromethane which has not yet been compressed is then greatly over-initiated (i.e., it occurs with a velocity higher than the steady-state value), and the detonation front rapidly decays to its normal steady-state value. Thus, with reference to Time Zones III and IV in Figure 1, a small portion of the explosive will be consumed by a detonation front moving at a hypervelocity before steady state is achieved. This general picture now explains the detonation steps in PETN (Reference 1). Additional support for this general description of the detonation-initiation process comes from the recent work by Hubbard and Johnson (Reference 6). Calculations of the shock-initiation detonation conditions utilizing time-dependent one-dimensional hydrodynamic equations with an Arrhenius form of chemical-energy release indicate the formation of a hypervelocity reaction wave behind the initiating shock front.

REFERENCES (APPENDIX)

1. T. E. Holland, A. W. Campbell, and M. E. Malin, J. Applied Phys., 28, 1212 (1957).

2. M. A. Cook, D. H. Pack, and W. A. Gey, Seventh Symposium (International) on Combustion, London, Butterworths, 1959, p. 820.

3. M. A. Cook, R. Keyes, and A. S. Filler, Trans. Faraday Soc., 52, 363 (1955).

4. R. F. Chaiken, "The Kinetic Theory of Detonation of High Explosives," M. S. Thesis, Polytechnic Institute of Brooklyn, 1958; also submitted to the Eighth Symposium (International) on Combustion, Pasadena, California, 1960.

5. A. W. Campbell, M. E. Malin, and T. E. Holland, J. Applied Phys., 27, 963 (1956).

6. H. W. Hubbard and M. H. Johnson, J. Applied Phys., 30, 765 (1959).

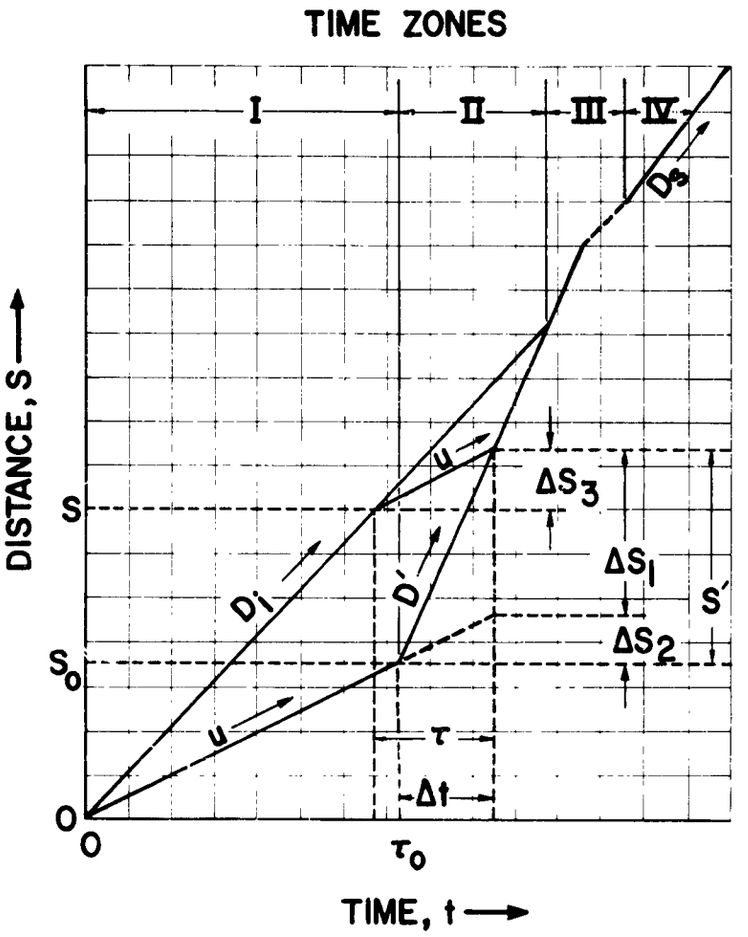

SPACE-TIME PLOT OF WAVE PROPAGATION UPON SHOCK INITIATION OF DETONATION

D_i = INITIATING SHOCK VELOCITY
u = VELOCITY IMPARTED TO THE MASS BY D_i
D' = "HYPERVELOCITY" WAVE VELOCITY
D = STEADY-STATE DETONATION VELOCITY

360-0038

Figure 1
Appendix

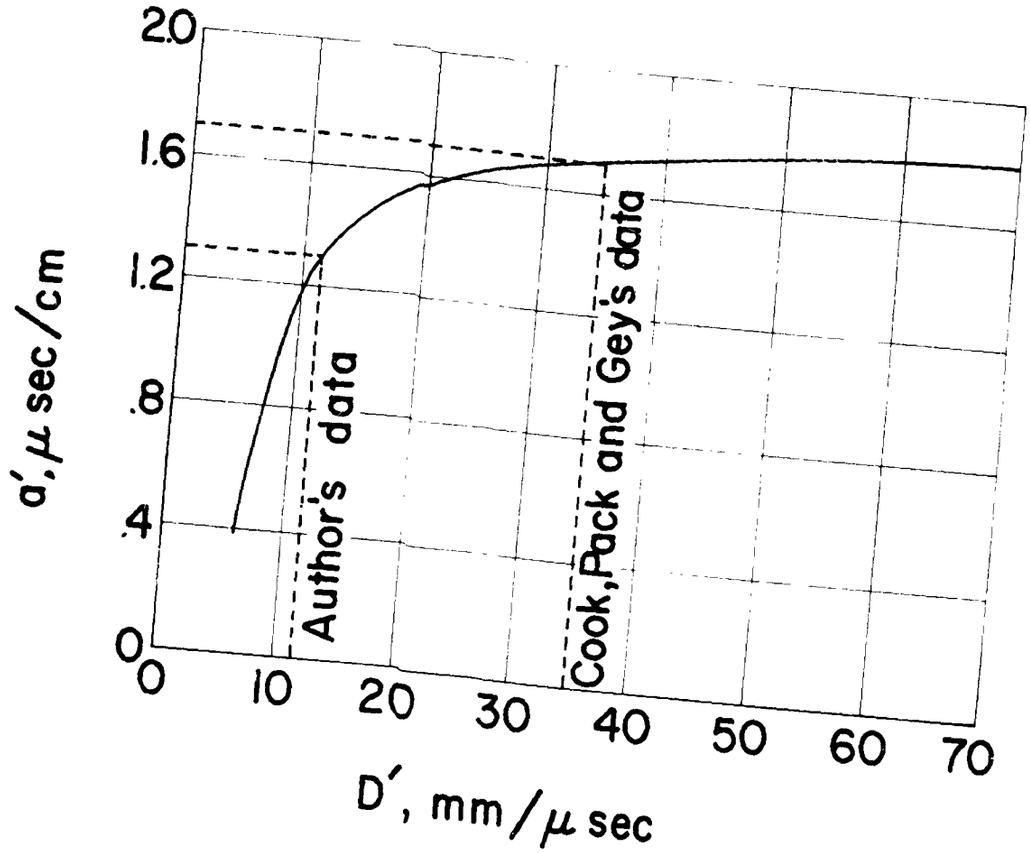

PLOT OF a' vs. D'

$a' = (D'/D_i - 1) / (D' - u)$

$D_i = 5.3$ mm/μ sec

$u = 2.4$ mm/μ sec

360-0037

Figure 2
Appendix

Report No. 1772

DISTRIBUTION LIST

	No of Copies
Head, Propulsion Chemistry Branch Office of Naval Research Washington 25, D. C. Attn: Code 426 VIA: BUWepsRep., Azusa	7
BuWepsRep., Azusa	1
SPIA List (15 June 1959)	As required
Internal	23